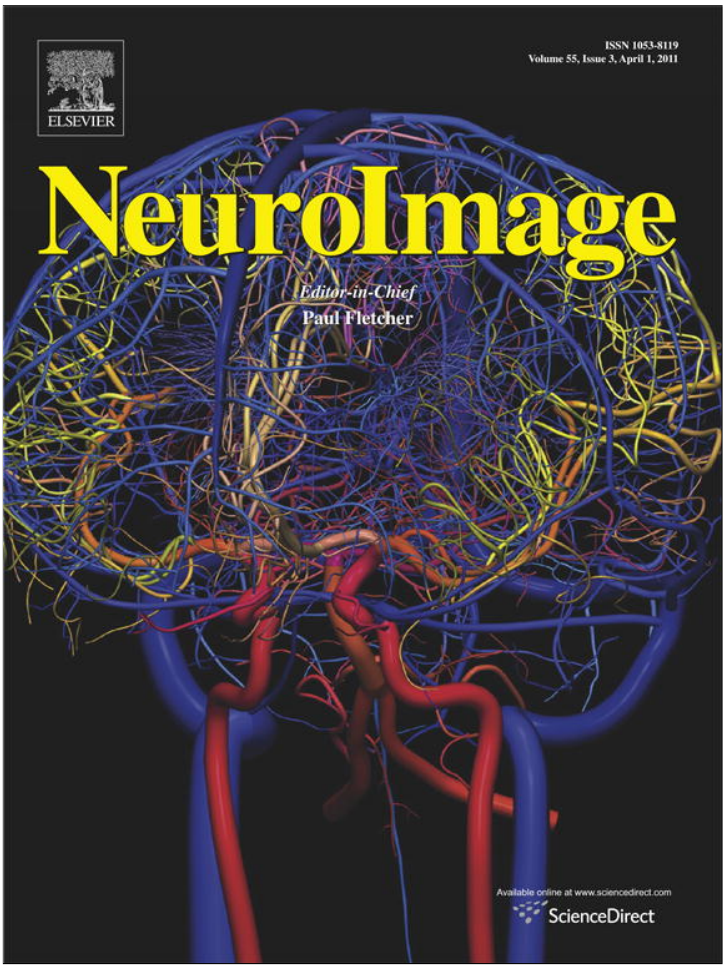

NeuroImage 55 (2011) 1189–1199

Contents lists available at ScienceDirect

NeuroImage

journal homepage: www.elsevier.com/locate/ynimg

Principles of recovery from traumatic brain injury: Reorganization of functional networks

Nazareth P. Castellanos [a,*], Inmaculada Leyva [b,c,*], Javier M. Buldú [b,c], Ricardo Bajo [a], Nuria Paúl [d], Pablo Cuesta [a], Victoria E. Ordóñez [a], Cristina L. Pascua [e], Stefano Boccaletti [f], Fernando Maestú [a], Francisco del-Pozo [a]

[a] Cognitive and Computational Neuroscience Laboratory, Centre for Biomedical Technology (CTB), Technical University of Madrid and Complutense University of Madrid, Spain
[b] Complex Systems Group, Universidad Rey Juan Carlos, Fuenlabrada, Spain
[c] Laboratory of Biological Networks, Centre for Biomedical Technology (CTB), Technical University of Madrid, Spain
[d] Department of Psychiatric and Medical Psychology, Medicine School, Complutense University of Madrid, Spain
[e] Centre of Brain Injury Treatment LESCER, Madrid, Spain
[f] CNR-Institute for Complex Systems, Florence, Italy

ARTICLE INFO

Article history:
Received 19 July 2010
Revised 1 December 2010
Accepted 16 December 2010
Available online 29 December 2010

Keywords:
Magnetoencephalography (MEG)
Functional connectivity
Graph theory
Traumatic brain injury (TBI)
Plasticity

ABSTRACT

Recovery after brain injury is an excellent platform to study the mechanism underlying brain plasticity, the reorganization of networks. Do complex network measures capture the physiological and cognitive alterations that occurred after a traumatic brain injury and its recovery? Patients as well as control subjects underwent resting-state MEG recording following injury and after neurorehabilitation. Next, network measures such as network strength, path length, efficiency, clustering and energetic cost were calculated. We show that these parameters restore, in many cases, to control ones after recovery, specifically in delta and alpha bands, and we design a model that gives some hints about how the functional networks modify their weights in the recovery process. Positive correlations between complex network measures and some of the general index of the WAIS-III test were found: changes in delta-based path-length and those in Performance IQ score, and alpha-based normalized global efficiency and Perceptual Organization Index. These results indicate that: 1) the principle of recovery depends on the spectral band, 2) the structure of the functional networks evolves in parallel to brain recovery with correlations with neuropsychological scales, and 3) energetic cost reveals an optimal principle of recovery.

Introduction

Traditionally, localizationist and holist views of brain function have exclusively emphasized either functional segregation or functional integration among components of the nervous system. While segregation indicates a high functional specialization of each brain region, integration highlights the idea of a global structure and cooperative behaviour. Neither of these views alone adequately accounts for the multiple levels at which interactions occur during brain functioning. Modern views conceive the human brain as having the capacity to conjoin local specialization with global integration (Tononi et al., 1994). Under this framework, the study of brain functioning is based on the idea that the brain is a complex network of complex systems with abundant interactions between local and distant areas (Singer, 1999; Varela et al., 2001; Fries, 2005; 2009; Singer, 2009). An approach to understand the dynamical nature of the links between neural assemblies could be functional connectivity (Friston et al., 1994), which refers to the statistical interdependencies between physiological time series recorded in various brain areas (Aertsen et al., 1989). Functional connectivity is, then, an essential tool for the study of brain functioning and the implications of the deviation from healthy patterns is a much debated question recently (Schnitzler and Gross, 2005; Guggisberg et al., 2008). Functional connectivity patterns have been proved to be altered by brain injury but, could they also reflect the capability of brain to compensate for such injury? One could think that it is possible, since brain plasticity produces changes at multiple levels of neuronal reorganization, from synapses to cortical maps and large-scale neuronal networks (Buonomano and Merzenich, 1998). Studies of the changes which occurred in the functional connectivity patterns after brain tumor rejections (Douw et al., 2008), recovery from capsular stroke (Gerloff et al., 2006) or traumatic brain injury (Castellanos et al., 2010) are some examples of the way the brain reorganizes after lesion. However, little is known about the principles governing the structural reorganization of functional networks after an acquired brain injury and during recovery.

* Corresponding authors. N.P. Castellanos is to be contacted at Laboratory of Cognitive and Computational Neuroscience, Centre of Biomedical Technology (CTB), Universidad Politécnica de Madrid, Campus de Montegancedo, 28660 Madrid, Spain. I. Leyva, Complex Systems Group, Universidad Rey Juan Carlos, Camino del Molino s/n, 28943 Fuenlabrada, Madrid, Spain.
E-mail address: nazareth@pluri.ucm.es (N.P. Castellanos).

1053-8119/$ – see front matter © 2010 Elsevier Inc. All rights reserved.
doi:10.1016/j.neuroimage.2010.12.046

Taking this into account, the study of brain injury and its recovery can be covered from this perspective. Traumatic brain injury (TBI) is one of the possible forms of acquired brain injury and origin of mortality and disability around the world (Cullen et al., 2007), leaving motor and, specially, cognitive deficits. Consequently, rehabilitation strategies to enhance the recovery of such deficits are needed (Cicerone et al., 2000, 2005), and are designed attempting to take full advantage of plasticity. Since cognitive functions require functional interactions between multiple brain regions (Bressler, 2002), the alteration of functional connectivity patterns after TBI could underlie both cognitive deficits and its recovery.

The general operating principle governing recovery can be quantitatively characterized by using the framework of complex network analysis, also called the graph theory (Bullmore and Sporns, 2009; Bassett and Bullmore, 2009; He and Evans, 2010; Stam, 2010). Graph theoretical analysis is being currently used to capture the global structure of the neural system and the interplay between segregation and integration. Within this framework, the recorded brain sites and the connections between them represent, respectively, the nodes and the links of the network (Boccaletti et al., 2006). The small-world architecture seems to be the key common feature shared by many complex systems (Watts and Strogatz, 1998) and there is evidence that structural and functional brain networks show this kind of organization (Gong and Zhang, 2009; Palva et al., 2009; Stam et al., 2009; Stam, 2010). Small-word structure is characterized by a pattern of dense local connectivity (clustering) and a small amount of distant connections that reduce the overall distance between nodes (path length). This property has been associated with efficiency in information transmission and parallel processing providing a model to better understand the interchange of information in the brain. However, an appropriate functioning of the network should balance this efficiency in transmission with the energy consumed in the process. For this purpose, certain network parameters are related with the energetic demand for the network maintenance. In this sense, the energetic cost *EC* of the network is especially meaningful, since it measures whether close or distant nodes are exchanging information (by measuring their correlations). The maintenance of correlations at a long distance is more energetically demanding and will lead to higher values of the energetic cost.

In the last few years, the idea of studying the properties of the brain networks applying the concepts of the graph theory has been used with healthy and pathological states of the brain. Palva et al. (2009, 2010a,b), in the context of a visual working memory maintenance task, showed that the networks associated to the alpha and beta bands were more clustered and small-world like but had smaller global efficiency than networks in delta, theta and gamma bands. In this case, they considered the topological efficiency, which can be measured as the inverse of the shortest path between nodes (Latora and Marchiori, 2001). In a neurological condition such as Alzheimer disease, Stam et al. (2009) showed decreased clustering coefficient and path length in the alpha band. Additionally, these authors showed, by means of a computational model, that changes in the network structure of the alpha band are better explained by a "targeted attack" model, indicating that highly connected neural "hubs" may be especially at risk in this disease. On the other hand, suboptimal economical properties of the human brain network have been shown to be related to an impaired accuracy of a working memory task in the beta band in schizophrenia patients (Basset et al., 2009). Alterations in beta band-based long-distance connections seem to be consistent with the disconnection syndrome model.

In this work we aim to address three well related questions: a) Could graph theory capture and quantify the alteration that occurred after TBI and its recovery? b) Are the structural parameters evolving parallel to the observed cognitive recovery in patients after neuropsychological rehabilitation? and c) Can we gain information about how the damage is affecting the functional network from the topological parameters? To address these questions we designed a study where patients underwent resting-state MEG recordings at two moments: a) a few months following the occurrence of a TBI and b) after a rehabilitation therapy. Results were compared with a control group of the same features. Functional connectivity patterns were estimated by means of wavelet-coherence and graph theory-based parameters were calculated. Next, we tested two theoretical models based on evolutionary networks in order to describe the changes observed during the recovery of the functional networks. We hypothesize that the network parameters after rehabilitation would restore to control ones, i.e., plasticity leads to network reorganization during recovery that could be carried out by means of restoration to the optimal topology. In order to test whether the rewiring of the network is related with its cognitive function, we correlate changes in topological parameters with changes observed in neuropsychological test scores. Fig. 1 summarizes the steps followed in order to obtain the functional networks and the topological parameters under evaluation.

Materials and methods

Patients

The dataset is composed of 29 subjects. These participants were divided into two groups: 15 TBI patients and 14 healthy controls. TBI patients were recruited from a rehabilitation centre where they had been referred in order to undergo a neuropsychological rehabilitation program. All patients showed severe cognitive impairments in several domains such as attention, memory and executive functions. The mean age of the patients was 32.13 years (range 18–51) and their mean level of education was 14 years (range 8–17). Time since injury at the beginning of the study ranged from 4 to 6 months (5 months average) and neuropsychological rehabilitation program lasted for a period between 7 and 12 months according to each patient's individual evolution (mean of 9.4 months). The healthy control group was chosen taking into account the demographic characteristics of the experimental group (mean age, 31.9; mean educational level, 15.8), not being statistically different. Exclusion criteria for the selection of all participants included previous medical history of psychiatric disease, extended psychoactive drug consumption and severe sensory or comprehension deficit. To evaluate neurophysiological and behavioural functioning, participants underwent two types of procedures: MEG recordings and neuropsychological assessment. TBI patients had MEG recordings and neuropsychological assessment before and after the neuropsychological rehabilitation program (hereafter called "pre" and "post" rehabilitation) whereas healthy controls were evaluated only once. We are aware that in longitudinal studies that test the evolution after brain injury, healthy controls need to be scanned at the same time interval as patients. However, it has been demonstrated that significant brain functioning and cognitive changes would not occur in healthy people in less than one year (Damoiseaux et al., 2006; Beason-Held et al., 2009). Moreover, recent results obtained with MEG (Deuker et al., 2009) have shown that the reproducibility of graph metrics in human functional networks shows a good reliability, especially at lower frequencies. All participants or legal representatives gave their written informed consent to participate in the study that was approved by the local ethics committee. Rehabilitation program for patients was conducted in individual one-hour sessions for three to four days a week. Also, neuropsychological assessment of both groups, patients and control people, was composed of tests in order to establish their cognitive status about attention skills, memory processes, language, executive functions and visuo-spatial abilities (for a more detailed description see Castellanos et al., 2010).

MEG recordings

Magnetic fields were recorded using a 148-channel whole-head magnetometer (MAGNES® 2500 WH, 4-D Neuroimaging) confined in a magnetically shielded room. Raw data were submitted to a noise

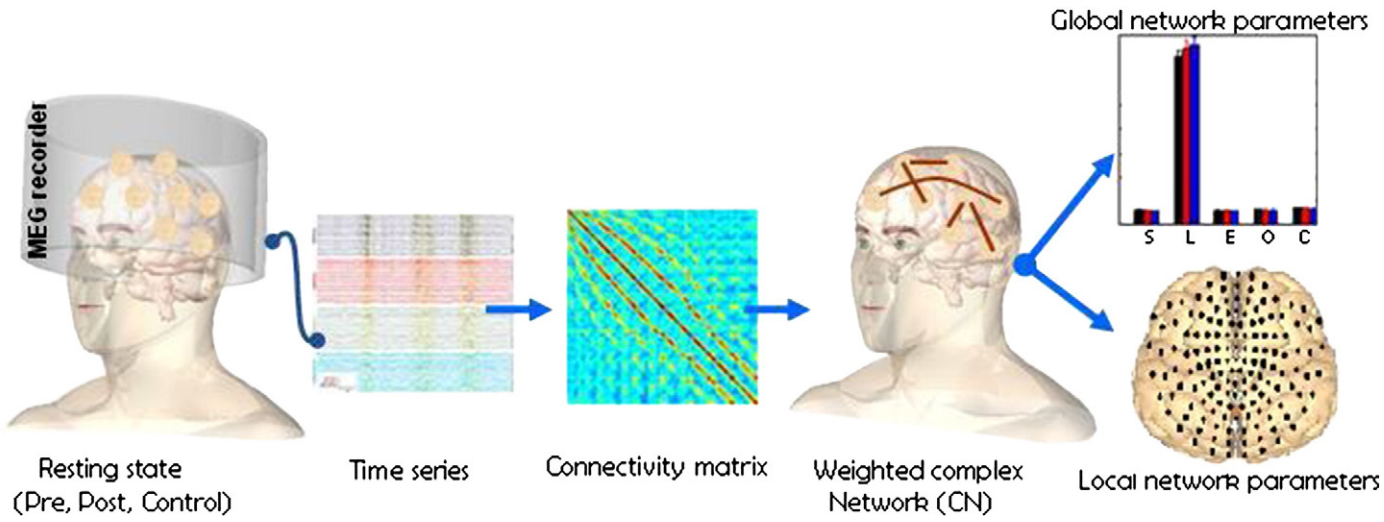

Fig. 1. Illustrative figure showing the experimental protocol and hypothesis to be tested in this work. We measure the magnetoencephalographic activity of 29 individuals (15 TBI patients and 14 healthy subjects) during resting state. Recordings of the TBI group are obtained after the injury and repeated after the cognitive therapy. Time-series obtained from the 148 channels of the magnetometer are filtered to avoid artefacts. Next, wavelet-coherence is calculated in order to obtain the coherence matrix. Complex network parameters are extracted from the weighted matrix. Two kinds of parameters are calculated: a) global parameters of the network: average strength *S*, shortest path length *L*, efficiency *E*, energetic cost *EC* and clustering *C*; and b) local parameters of each node: participation coefficient P_i and within-module-degree z_i.

reduction procedure that uses simultaneous recording from nine reference channels that are part of the magnetometer system. Thereafter, recorded signals were submitted to a band pass filter of [0.3,50] Hz. Magnetic fields were measured during resting state with opened-eyes condition, at a sampling frequency of 169.45 Hz. Time windows without artefacts were visually selected by an experienced investigator, to reach segments of up to 12 s length.

Functional connectivity and graph analysis

Graph measures are based on the functional connectivity matrices calculated by means of global wavelet coherence, a time-averaged normalized measure of association (Torrence and Compo, 1998; Grinsted et al., 2004). Wavelet-coherence between all combinations of the 148 magnetometers was calculated, providing a 148×148 matrix. Then, we evaluated the statistical significance level of the coherence values by using a surrogate data test (Theiler et al., 1992; Schreiber and Schmitz, 2000; Korzeniewska et al., 2003) with Monte Carlo simulation to establish a 95% confidence interval and to avoid spurious couplings. Those weights that did not pass the statistical test were set to zero. For each individual, matrices were calculated in the delta ([1,4] Hz), theta ([4,8] Hz), alpha ([8,12] Hz) and beta ([12,30] Hz) bands. The results of functional connectivity changes of this particular dataset have been recently published by Castellanos et al. (2010).

In our study, we consider the matrices as complex networks, where nodes are the recording sites (148 magnetometers) and links are obtained from the wavelet coherence after validation by means of surrogates. We use weighted matrices, that is, we have not thresholded the matrices to obtain a binary projection. In this way, we ensure that all the possible information is held. Matrices are close to be fully connected, since the fraction of non-significant links (whose weight is set to zero) is very low. As shown by Nakamura et al. (2009), the analysis of weighted networks, instead of their unweighted versions, gives better results when comparing the network structure of different groups of individuals. The features of the resulting networks can be characterized by various graph-based measures (for a recent review see Bullmore and Sporns, 2009), which can be compared between the pre, post and control groups. In what follows, we give a description of the parameters used in this work.

The average network strength S quantifies how synchronized is the whole network,

$$S = \frac{1}{N}\sum_{\substack{i,j \\ i\neq j}} w_{ij} \tag{1}$$

where *N* is the number of nodes, and w_{ij} is the weight between nodes i and j.

In a binary matrix, the shortest path length L is the minimum number of nodes that must be traversed to go from one node to another. In a weighted matrix, we have to take into account the different weights of the links, considering that, the higher the weight, the shorter the topological path between two nodes. Therefore, the topological length l_{ij} of the link between nodes *i* and *j* is defined as the inverse of the link weight, $l_{ij} = 1/w_{ij}$. However, when computing *L* for weighted matrices, the shortest length between a pair of nodes may not be a direct link, since there could exist a shorter path by combining two or more alternative links. Therefore, we computed the minimal shortest path p_{ij} between all pair of nodes (Dijkstra, 1959). Next, we define the average shortest path *L* of the matrix as:

$$L = \frac{1}{N(N-1)}\sum_{\substack{i,j \\ i\neq j}} p_{ij} \tag{2}$$

where L is a measure of how well connected the network is.

The inverse of the shortest path length is related (but not equal) to the global efficiency E of the network (Latora and Marchiori, 2001), which is calculated as:

$$E = \frac{1}{N(N-1)}\sum_{\substack{i,j \\ i\neq j}} \frac{1}{p_{ij}} \tag{3}$$

As explained by Latora et al., the global efficiency E is a good indicator of how well the information is transmitted in a parallel system: the higher the efficiency, the better the information flows.

The previously defined l_{ij} is the topological distance between two nodes but, as long as the brain connectivity involves energy, the physical Euclidean distance between any pair of nodes $\left(d_{ij} = \sqrt{(x_i - x_j)^2 + (y_i - y_j)^2 + (z_i - z_j)^2}\right)$ has important implications

for the energetic consumption, since the longer the connection, the more the energetic consumption. To take this factor into account, we define the energetic cost EC as the average of the outreach of the nodes (Dall'Asta et al., 2006):

$$EC = \frac{1}{N(N-1)} \sum_{\substack{i,j \\ i \neq j}} w_{ij} d_{ij} \tag{4}$$

which simultaneously accounts for both topological and physical parameters. High values of energetic cost EC are obtained when physically long-distant connections (high d_{ij}) also have high weights (high w_{ij}), since the combination of both features leads to high energetic consumption. Notice that EC is more physically relevant than cost-efficiency (Achard and Bullmore, 2007), where only the topological distance is considered, and therefore it does not reveal the energetic effort of the network to get synchronized.

Finally, in order to acquire knowledge about the local state, we use the weighted clustering coefficient C (Stam et al., 2009). This parameter measures the likelihood that neighbours of a node will also be connected between them. The weighted version of the clustering characterizes the tendency of nodes to form local clusters of synchronization:

$$C = \frac{1}{N} \sum_{i} \frac{\sum_{j,k} w_{ij} w_{jk} w_{ik}}{\sum_{j,k} w_{ij} w_{ik}} \tag{5}$$

These measures do not depend exclusively on the weights of the links, but also on the network structural organization. With the aim of quantifying changes in the network structure, we compare all measures to the corresponding average values of 100 surrogated random networks constructed from the original ones by randomly reshuffling the edge weights. In this way, we obtain the corresponding random values Lr, Er, ECr, and Cr, and next, we use them to normalize all parameters ($\hat{X} = X / X_r$). In this way, values of normalized parameters close to the unity ($\hat{X} \approx 1$) would indicate that the network has a similar structure to its random counterpart ($X \approx Xr$). On the contrary, the longer the distance to the unity, the less random the functional network is.

The above described measures are global characteristics of the network. However, some nodes may have more relevant topological roles than others in local and/or distant connections. In order to establish intra and inter lobe connections, MEG channels were grouped into frontal (F), central (C), right temporal (RT), left temporal (LT) and occipital (O) regions. Since we are interested in the relations between anatomical and functional networks, we have chosen the community division corresponding to the anatomical assignation commonly used in literature. This division has also the advantage of being related to the local segregation of cognitive features, whose improvement evaluation is the last goal of our study.

Local connections involve correlations within a certain brain area whereas non-local connections involve correlations between two different regions (F–C, F–RT, F–LT, F–O, C–RT, C–LT, C–O, RT–LT, O–RT, and O–LT). The relevance of each node can be described as the role that it plays in its own region (intra-region hub) or connecting different brain regions (inter-region hub). The within-module-degree Z measures how connected is a node compared to its own brain region. For a node i belonging to the brain region B (Guimerà and Amaral, 2005; Meunier et al., 2009), Z_i is given by,

$$Z_i = \frac{W_{Bi} - W_B}{\sigma W_i} \tag{6}$$

where W_{Bi} is the total local weight of the i node, W_B is the average local weight in the brain region B, and σW_i is the standard deviation of the local weights in the brain region B. Therefore, $Z_i \sim 0$ if node i has a local weight around the average value inside its community (lobe). Next, we calculate the participation coefficient P_i, which measures how a node i spreads its connections among all brain regions. The weighted version for a participation coefficient P_i of node i can be written as (Guimerà and Amaral, 2005):

$$P_i = 1 - \sum_{B=1}^{N} \frac{W_{Bi}}{W_i} \tag{7}$$

where W_i is the total weight of the links of node i. If most of the connectivity weights of node i are inside its own community, then P_i is small, and otherwise P_i approaches to 1 if node i has its links mostly distributed over the other communities.

Statistical tests

To increase the statistical power and reduce the effect of the non-Gaussian distribution, we normalize topological parameters by means of a logarithmic transformation (Gasser et al., 1982; Pivik et al., 1993). The log-transformed synchronization values are statistically analyzed by using a pairwise Kruskal–Wallis (U Mann–Whitney for 2 groups) to compare control, pre and post conditions. Next, the statistics are analyzed with Matlab statistical toolboxes. Associated p-values were thresholded at $p<0.05$ (see Brookes et al., 2005; Campo et al., 2010; Castellanos et al., 2010, for a similar statistical approach).

Results

Graph parameters changes

Can graph theory-based measures capture the alteration which occurred after a TBI and its recovery? And, can they describe the kind of changes in the network? To address these questions we quantified the changes which occurred in network parameters in the pre (after TBI) and post (after rehabilitation treatment) groups and their changes relative to the control group. In what follows, we concentrate in two spectral bands; delta ([1,4] Hz), and alpha ([8,12] Hz), since they are the bands where changes were statistically significant.

Table 1 summarizes the values of the absolute and normalized network parameters (of control, pre and post groups) and indicates those values that are statistically different form the control group. In Fig. 2 we plot the average distance (in percentage) of the graph measures of the pre and post groups to the control one. We observe that TBI affects the delta and alpha bands in opposite ways. In the delta band (Fig. 2A), there is an increase (~11%) of the overall network strength S after the TBI, which is a consequence of a higher synchronized activity between brain regions. After the rehabilitation therapy, the network strength recovers to a value that is only ~3% higher than the control group. Interestingly, changes observed in the rest of the network parameters are influenced by the increase of S. Since network weights have increased, distances between nodes are reduced and the network shortest path L decreases (~−8%). Again, the distance to control is higher after the TBI than after therapy, which reveals that patients are restoring to those values of the healthy group. The network efficiency E, energetic cost EC and clustering C behave in a similar way, with an increase higher than 8% in the pre group which is reduced in all cases after therapy. The increase of these three parameters is in accordance with the enhancement of the network strength S. In order to evaluate whether the changes in the network parameters are a consequence of the increase of S or there is reorganization in the network structure, we calculate the normalized network parameters. We can observe in Fig. 2C that the percentage of variation is in all cases lower than 0.5% and not statistically significant, despite that the changes in the absolute values are around 8% to 10%. This fact reveals that there are no significant changes in the network structure (neither after TBI nor after therapy), since normalization by the randomized version of the network is not sensitive to changes in the network strength S. The main conclusion is that the delta-band

Table 1
Absolute and normalized (^) network parameters for the control, pre (after TBI) and post (after therapy) groups.

δ	Control	Pre	Post
$S^{*\dagger}$	0.368 ± 0.014	0.408 ± 0.015	0.379 ± 0.024
$L^{*\dagger}$	2.84 ± 0.09	2.61 ± 0.08	2.80 ± 0.11
$E^{*\dagger}$	0.357 ± 0.012	0.390 ± 0.013	0.368 ± 0.021
$EC^{*\dagger}$	0.395 ± 0.016	0.438 ± 0.017	0.408 ± 0.027
C^{*}	0.395 ± 0.012	0.430 ± 0.013	0.410 ± 0.024

α	Control	Pre	Post
S	0.38 ± 0.03	0.352 ± 0.017	0.361 ± 0.012
L	2.64 ± 0.14	2.76 ± 0.08	2.70 ± 0.06
E	0.389 ± 0.019	0.37 ± 0.01	0.374 ± 0.008
EC	0.41 ± 0.03	0.375 ± 0.019	0.385 ± 0.013
C	0.427 ± 0.016	0.412 ± 0.008	0.416 ± 0.006

δ	Control	Pre	Post
$\hat{L}$	1.090 ± 0.007	1.0865 ± 0.012	1.090 ± 0.011
$\hat{E}$	0.922 ± 0.006	0.927 ± 0.011	0.924 ± 0.001
$\hat{EC}$	0.922 ± 0.003	0.922 ± 0.006	0.924 ± 0.005
$\hat{C}$	1.022 ± 0.002	1.024 ± 0.003	1.027 ± 0.006

α	Control	Pre	Post
$\hat{L}^{*}$	1.05 ± 0.01	1.079 ± 0.007	1.073 ± 0.007
$\hat{E}^{*}$	0.951 ± 0.009	0.932 ± 0.006	0.938 ± 0.009
$\hat{EC}$	0.918 ± 0.004	0.914 ± 0.004	0.916 ± 0.003
$\hat{C}^{*\cdot}$	1.0146 ± 0.0013	1.022 ± 0.003	1.022 ± 0.005

The left column corresponds to delta band and the right column to the alpha band. Network parameters are: average strength *S*, shortest path *L*, efficiency *E*, energetic cost *EC* and clustering *C*. The statistical significance ($p<0.05$) of each mean value is indicated by symbols: (*) statistical difference between pre and control, (†) statistical difference between pre and post and (•) statistical difference between post and control. Colours of the post values correspond to: (green) total recovery, achieved when pre ≠ control, post ≠ pre and post = control, (blue) partial recovery, obtained when pre ≠ control, post = control but post = pre, and (red) not recovered, pre ≠ control, but post ≠ control and post = pre. We can see that statistical differences are only obtained at the absolute values of the delta band and the normalized values of the alpha band.

functional network increases its strength after TBI, but the structure of the functional network remains the same. After therapy, absolute values of the network parameters recover in the direction of the control group, despite that recovery is not complete. Note that the maintenance of the global structure does not necessarily involve that the distribution of weights is constant: weights may have changed from node to node, but without a significant impact in the statistical properties of network structure.

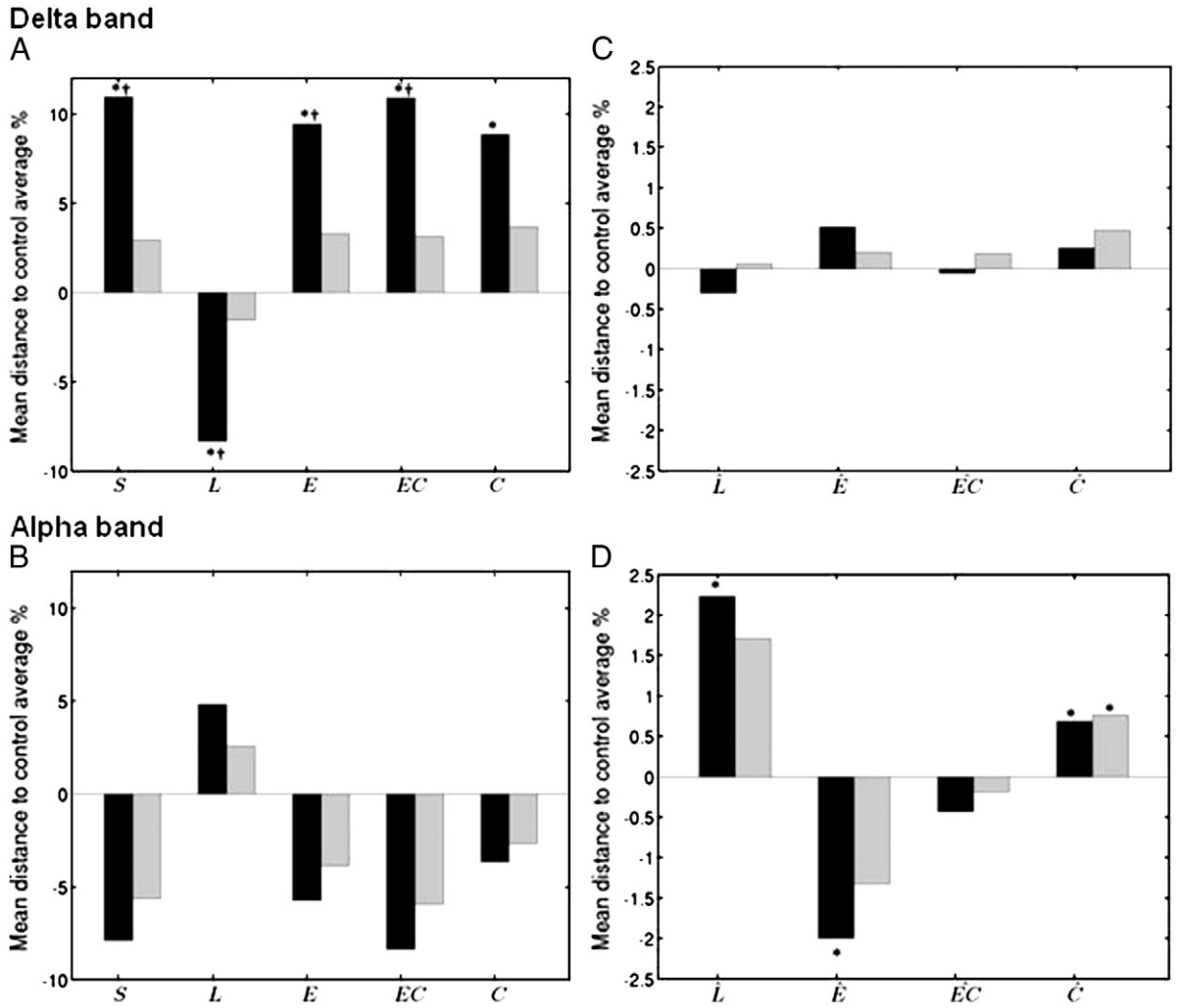

Fig. 2. Differences of the network parameters of the pre (black bars) and post (grey bars) group with regard to the control group. Plots A and C are the absolute and normalized network parameters for the delta band, while B and D are for the alpha band. The distance-to-control of all parameters is given by $\%X = \frac{X_{pre/post} - X_{control}}{X_{control}} \times 100$. The statistical significance ($p<0.05$) of each value is indicated by symbols: (*) statistical difference between pre and control, (†) statistical difference between pre and post and (•) statistical difference between post and control.

Interestingly, changes in the alpha band go in the opposite direction (see Figs. 2B and D). Despite that the absolute differences in the control group are lower than in the delta band, four of the topological parameters suffer a variation higher than 5%. In this case, it is a decrease in the network strength S that determines the modification of the network parameters. After the TBI a reduction of the synchronized activity in the alpha band leads to a decrease of the S parameter around 8%. As a consequence, the shortest path between nodes increases (~5%) and the rest of the network parameters decrease. Despite that the changes in the mean values are important, they do not pass the statistical test. Nevertheless, we can extract additional conclusions from the analysis of the normalized parameters. If we compare Fig. 2C (normalized delta band) and D (normalized alpha band), we see that despite that the changes in the absolute values are lower in the alpha band, the variation of the normalized parameters is much higher, especially in the shortest path length L and the global efficiency E. In addition they are statistically significant ($p<0.05$), as can be observed in the values given in Table 1. This fact indicates that TBI leads to a reorganization of the functional network, but it is only statistically reported in the alpha band. After the therapy, network parameters evolve in the direction of the control group, but, as can be seen in Figs. 2B and D, the recovery is not complete. Nevertheless, there are no statistical differences in L, E and EC parameters between the post and control groups, and only the clustering C shows statistical differences between the post-therapy patients and healthy individuals.

Correlation between topological parameters and neuropsychological test scores

Neuropsychological outcomes, as described in Castellanos et al. (2010), show a general trend of improvement, in comparison between pre and post conditions, as well as with the control group. These results are indicative of cognitive recovery of patients in the study with a rapprochement to healthy control group for post condition in all neuropsychological tests. However, although they recovered in a significant way, did not reach a complete reestablishment of all the cognitive processes.

Further post-hoc analyses were performed to explore whether neuropsychological test score changes in patients were related to changes in topological measures, in delta and alpha bands. Subsequently, Pearson's correlation coefficients were calculated and t-tests were performed ($p<0.05$). The topological changes showing significant correlations are path length, L, in delta frequency band and, normalized global-efficiency ($\hat{E}$), in alpha frequency band.

A positive correlation between the changes underwent from pre to post condition path length, L, and Performance IQ of WAIS-III changes is found, $R=0.52$ (Fig. 3). Positive correlation means that those patients who increased L in the delta band during the recovery are those that showed greater improvements in their Performance IQ scores. This positive correlation agrees with the progressive increase of L values from pre to control reference, as shown in Fig. 2. Additionally, a positive correlation between post and pre network normalized global efficiency, $\hat{E}$, and Perceptual Organization Index of WAIS-III changes is found, $R=0.73$ (Fig. 3B). This positive correlation means that those patients who increased alpha-based normalized global efficiency are those that showed greater improvements in their W-POI values. As the bar diagram shows, pre $\hat{E}$ values are lower than control ones. So a decrease of $\hat{E}$ values from pre to post is needed for an approaching the control reference, in agreement with the positive correlation found.

Analysis of node performance

The above studied parameters define the global properties of the whole network. However, spatial information such as brain region localization of changes could help us to understand the recovery process after damage. For this purpose we grouped MEG channels into five brain regions, each one corresponding to a brain lobe [frontal (F), central (C), right temporal (RT), left temporal (LT) and occipital (O)], and we defined local connections (within a brain area) and distant connections (between different brain areas). Considering both local and distant connections, a degree of participation could be defined for each node (MEG sensor in this case). The within-module degree (Z) and the participation coefficient (P) quantify how connected is a node within its own community (local hub) and between brain areas (connector hub), respectively. In order to know which nodes are more involved in the recovery, we define "recovered nodes" in terms of their changes in Z and P. Recovered nodes are those whose Z and P in pre condition are statistically different from both control and post values, whereas both parameters in post condition are statistically similar to control reference. Fig. 4 shows the "recovered nodes" in delta and alpha band-based networks from both local- (red circles) and distant-connector (black circles) perspective. In the delta band-based network, the "recovered nodes" are mainly concentrated in central, right temporal and occipital areas. Both local and distant hubs take part in the recovery. Interestingly, the number of recovered nodes (34) is three times higher than the not recovered ones (10), indicating the efficacy of the recovery process in this band. In the alpha band, we do not find a predominance of the recovered nodes (16) over the not recovered ones (18). Interestingly, the recovery of local activity (black nodes) is much lower (5) than the recovery of the activity between distant regions (11). On the contrary, nodes which

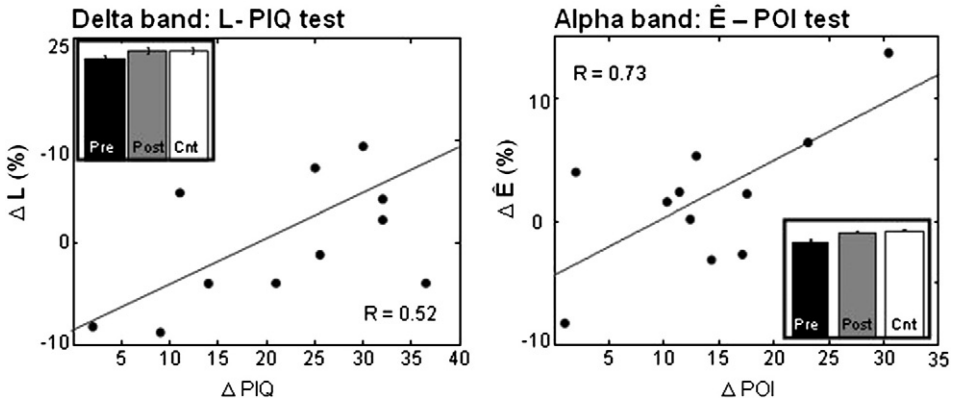

Fig. 3. Correlations between topological changes and neuropsychological test score changes. A) Changes in the average path length in delta band positively correlate with changes in PIQ (Performance IQ) test score. The increase observed in L from pre to post condition (Fig. 2) agrees with the positive sign of correlation. B) Changes in the normalized cost positively ($\hat{E}$) correlate with changes in POI (Perceptual Organization Index) test score. The increase observed in $\hat{E}$ from pre to post condition (Fig. 2) agrees with the positive sign of correlation. Bar diagrams show the average of the PIQ and POI scores for control, post and pre condition. * codes a statistical differences ($p<0.05$).

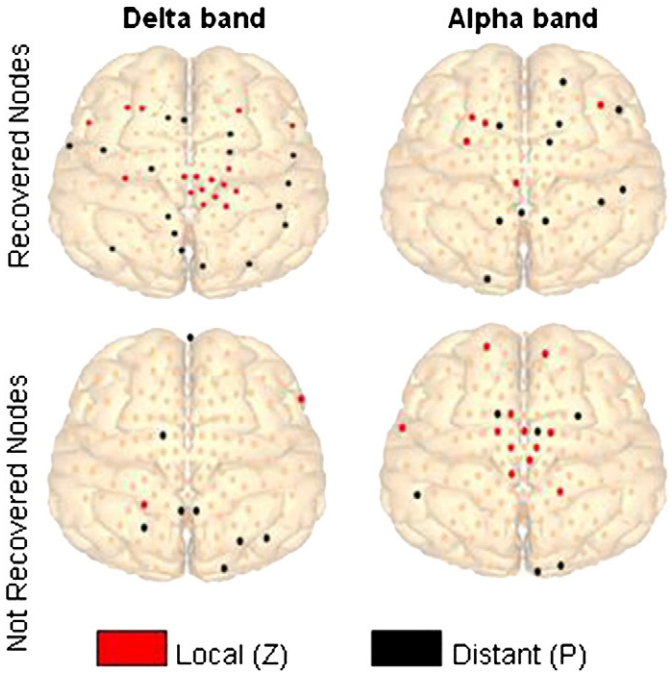

Fig. 4. Recovered nodes, defined as those whose within-module degree Z (local importance) and participation coefficient P (connector role between lobes) in pre condition is statistically different to both control and post participation, whereas at the same node the post condition is statistically similar to control reference. Not recovered nodes are those whose P and Z parameters in the control group are statistically different between both pre and post groups, whereas P and Z in post condition are statistically similar to pre rehabilitation condition. Red nodes represent recovery/no-recovery at the local activity whereas black nodes account for long-range connections.

did not recover their local role are more present (12 out of 18) than the nodes that did not restore their long range connections.

Modelling functional networks changes: the targeted model

The differences in the network structure observed in the alpha band make us to propose a model that modifies the average strength and simultaneously introduces changes in the structure. With this aim, we hypothesize that the changes in the weight of the links due to recovery are not homogeneous in percentage, but affect each link in a different ratio, proportionally to the weight (stronger edges are more sensitive to be recovered than weak ones). This effect may modify the network in two directions and could be modelled by two different perspectives: a) a model which enhances the weight differences between links, such that at each time step high weighted links increase their structural role (called *contrasting-model*), or on the contrary, b) a model which reduces the differences, leading to a homogenization of the weights and, therefore, reducing the hierarchical structure (called *unifying-model*).

To implement both hypotheses, we design a model that takes the real pre-therapy matrix as the initial data, $\boldsymbol{A}_0^i$ at $t=0$. For each time step t, the evolution of the matrix is calculated as $\boldsymbol{A}_t^i = \boldsymbol{T}^i \boldsymbol{A}_{t-1}^i$, where $\boldsymbol{T}^i$ is a matrix calculated as:

$$\boldsymbol{T}^i = m\left[\frac{\boldsymbol{A}_0^i}{\max(\boldsymbol{A}_0^i)}\right] + b \tag{8}$$

Contrasting-model (T_+): The goal of this model is enhancing those links with higher initial weights, being the coefficients $m_i = \frac{1-k}{1-\min(A_0^i)}$ and $b = \frac{k-\min(A_0^i)}{1-\min(A_0^i)}$. At every step, the global weight is reduced, but not homogeneously, since each link is multiplied by a different value ranging in the interval $[k,1]$, with $k<1$, being 1 the highest weight and k the minimal. This leads to an increase of the relative difference between higher and lower weights along the evolution.

Unifying-model (T_-): Alternatively, if we want to reduce the relative differences between weights, the coefficients of Eq. (8) can be changed to $m_i = \frac{k-1}{1-\min(A_0^i)}$ and $b = \frac{1-k\cdot\min(A_0^i)}{1-\min(A_0^i)}$, and we obtain opposite effects: the global average strength of the matrix decreases and, in addition, the relative differences between link weights are reduced at each time step.

In Fig. 5 we show the results of these two versions of the targeted model. In Figs. 5A and B the evolution of the network parameters for the delta band can be observed, both for T_+ (cyan traces) and T_- (magenta traces), being $k=0.99$. The parameter k has been chosen to fit the average strength S of the post-therapy experimental values after 30 time steps. It can be seen that for the global parameters (Fig. 5A) in the delta band the evolution due to T_+ and T_- still fits with the experimental values. However, the targeted model fails to reproduce the stability of the normalized measures observed in the experimental data (Fig. 5B). In Figs. 5C and D we show the results of the targeted model for $k=1.0025$ in the alpha band, both for T_+ and T_-. The absolute values of the network parameters (Fig. 5C) show a good resemblance to the real evolution, but the important point is the fact that, in this band, the targeted model succeeds in reproducing the changes in the normalized measures (Fig. 5D), whose modification reflects the reorganization of the network structure. Specifically, we see that the main tendency of the structural changes is caught only by the T_+ version of the targeted model (cyan traces), the contrasting-model. These results point to the hypothesis that in the alpha band the structural reorganization after recovery corresponds to an increase of the strength in the most active links rather than in the rest of the edges. On the contrary, the unifying model T_-, which homogenizes the network, leads to an evolution of the network parameters in a direction opposite to the real changes (magenta circles of Fig. 5D).

Discussion

The aim of this work could be uniquely centred in testing whether recovery from traumatic brain injury has occurred or not. In this sense, our results can be interpreted as a positive improvement, in terms of approaching to control reference (as previously shown by Castellanos et al., 2010). However, the capability of the mathematical analysis introduced in the current study also allows studying the way plasticity process underlies recovery: following an evolution to healthy functional networks that implies an adjustment of the overall synchrony in the delta band and structural reorganization in the alpha band.

Our results show that delta and alpha are the bands where network changes are statistically significant. After TBI, the network strength S and the energetic cost EC are the most altered topological parameters, showing opposite changes in the delta (increase) and alpha (decrease) bands. After the cognitive therapy (post condition), topological parameters evolve in all cases to those of the control group, both in the alpha and delta spectral bands. Nevertheless, a reorganization of the network structure is only reported in the alpha band, while changes in the network parameters of the delta band can be explained as a consequence of the increase of the network strength S.

Although finding signs of recovery in theta and beta bands (data not shown), the statistical differences were not robust enough to be taken into account. Nevertheless, both theta and beta-based parameters of the pre group were more distant to the control reference than in the post group for almost all the topological measures.

In order to test if such measures, capturing global topological properties, evolve in parallel to the cognitive recovery observed in patients after therapy, we correlate topological with neuropsychological-

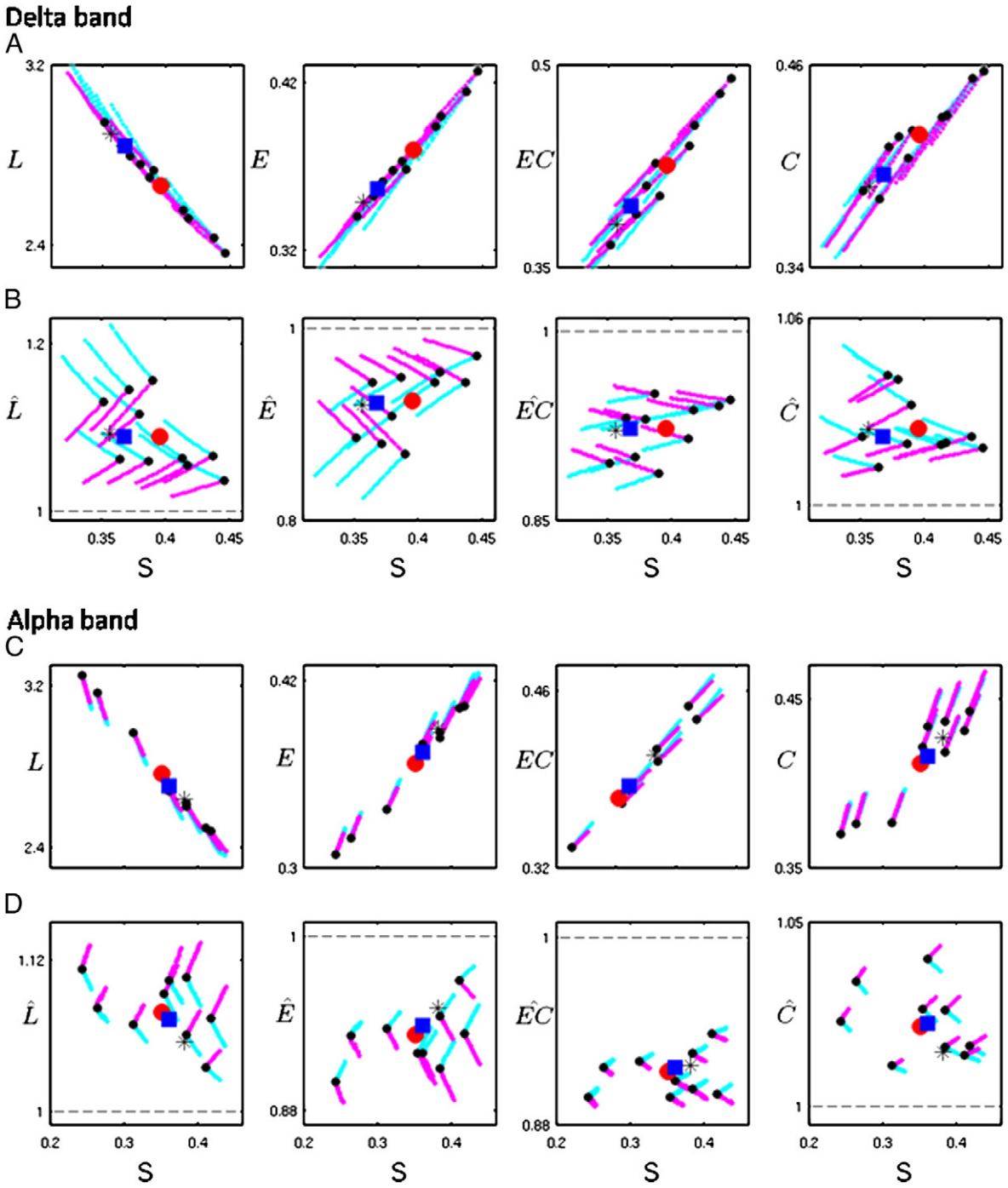

Fig. 5. Results obtained with numerical simulations of the targeted models T_+ (light-blue circles) and T_- (magenta circles). In all panels, the average parameters of the pre (red circle), post (blue square) and control (black star) groups are plotted. Panels A–B: Evolution of delta band network parameters (light-blue dotted lines) of pre-therapy patients, with the initial value before therapy in black dots: absolute values (A) and normalized values (B). Panels C–D: Evolution of alpha band parameters of pre-therapy patients (with the same colour code): absolute values (C) and normalized values (D).

test changes. We find correlations with some of the general scores of the WAIS-III test, specifically, a positive correlation between changes in delta-based path length (L) and those in Performance IQ score (PIQ), and a positive correlation between alpha-based normalized global-efficiency ($\hat{E}$) and Perceptual Organization Index (POI).

We note that the most altered parameters after TBI were in all spectral cases the network strength *S* and the energetic cost *EC*. The most pronounced changes are found in the absolute parameters of the delta band, where statistical differences arise between pre and control conditions but disappear in the post condition, unveiling the recovery of the original network structure. In this band, all graph-based parameters increase after TBI and reduce after therapy, approaching to control reference. The only exception is the network shortest path *L*, whose decrease is a consequence of the higher weights in the connections between brain regions. The pathological increase of slow rhythms is widely documented in the literature (Lewine et al., 1999; Bartolomei et al., 2006a,b; Lewine et al., 2007; Bosma et al., 2008). It seems that the increased delta-based connectivity in patients following a TBI reflects a generalized physiological malfunctioning which diminishes with cognitive recovery. A higher strength could

point out to a better transmission, but in fact the high levels of extra energetic cost reveal an overcharged network, unbalanced in the transmission versus energy consume trade-off. The impact of a TBI on alpha-based network produces, contrarily to delta network, a disconnection effect. Our results show that the alpha band network in the pre condition is characterized by a lower clustering and longer path length than control references, leading to a network with reduced transmission capabilities. This effect is corrected after the therapy, which approximates clustering and path length to those values of the control group. In addition, these changes are related to the improvement in neuropsychological test evaluation.

The approaching of post-patient's topological parameters to control reference can be interpreted as a recovery after the rehabilitation intervention. However, we are conscientious about the still opened debate on treatment effectiveness (Rohling et al., 2009; Cicerone et al., 2005). Changes observed on psychometric test of cognitive function after rehabilitation is commonly interpreted as a sign of effectiveness of the rehabilitation process (Park and Ingles, 2001). Results provided by neuroimage studies principally show spatially localized physiological changes. Due to the diversity of techniques and tasks used, and the absence of a control reference, the conclusions are heterogeneous (Kelly et al., 2006). The aim of this work could not be to test if changes observed at the neuropsychological or neurophysiological level are, or not, due to rehabilitation interventions. We are conscientious about the limitation due to the lack of a group of patients that have not received neurorehabilitation. However, the declaration of Helsinki establishes that a treatment that has been probed beneficial for patients should not be denied just by experimental reasons. Considering this limitation the current study can only provide evidence of the neurophysiological mechanisms underlying the process of neuronal plasticity after brain injury but does not pretend to be a measure of effectiveness of rehabilitation. However, the correlation between topological changes and improvement of the neuropsychological tests could be interpreted as evidence that network topology and cognitive recovery evolve in a simultaneous and related way after brain injury. Nowadays, the neuroscientific community using mathematically abstract frameworks, as graph theory, is debating "*how the parameters of complex brain networks relate to cognitive and behavioural functions? This will probably be a key focus of future work that might be combined with further studies of clinical disorders*" (Bullmore and Sporns, 2009). Our work points in this direction and it correlates network parameters with cognitive functions, for the first time, in patients suffering from TBI. Concerning other kind of studies, it has been probed very recently that intellectual performance is related to the overall connectivity network topology of the brain (Stam, 2010). In the work by Bassett and Bullmore (2009), the authors studied how the spectral topology of brain networks can be related to behavioural performance on cognitive task. They showed that superior working memory performance is associated with greater cost-efficiency at high frequency (beta band). The association of brain network architecture and cognitive functioning was also demonstrated by Li et al. (2009). On the other hand, anatomical brain networks estimated from MRI-DTI in healthy subjects showed high clustering and short path length (typical properties of small-world networks). The authors found that higher IQ is correlated with a larger number of connections, shorter path length and higher efficiency. Other works in anatomical networks, such as van den Heuvel et al. (2009), studied the association between how efficiently the regions of the brain are functionally connected and our level of intelligence. Very interestingly, they found : a) a positive correlation between the path length and intelligence quotient (IQ) and b) a positive association between the global efficiency (normalized) of the brain networks and intellectual performance. Micheloyannis et al. (2006) tested the neural efficiency hypothesis comparing the topology in healthy controls having few years of normal education with individuals with university degrees. They found that those people with university degrees exhibit less small-world properties in most frequency bands during a working memory task. Our results show that those patients who had more increases in delta-based path length (increase after TBI) are also those who showed greater improvements in Performance IQ scores. Performance IQ takes into account specific abilities related to executive functions, attention, praxis and memory process. These cognitive functions are commonly altered in TBI, and it is important to improve them for the patient's adaptation to social and work activities. We found that, interestingly, L is one of the topological parameters that correlate with IQ in previous studies, as mentioned before. Performance IQ takes into account complex abilities that, as stated by Stam et al., "*require the delicate cooperation of multiple specialized areas in the brain to allow optimal information processing*" (Stam, 2010). This optimal information processing, can be carried out by means of a short path length, which implies that any area of the brain can be reached in a small number of (topological) steps. The recovery of L (in terms of approaching to a healthy reference) could be, then, a remarkable parameter whose recovery implies an improvement in IQ scores. Additionally, those patients with higher increases of alpha-based normalized global-efficiency $\hat{E}$ (decreased after TBI), are those who showed greater improvement in the Perceptual Organization Index (POI), which is related to working memory and visual–spatial task. It is interesting to highlight that those cognitive scores that better correlate with topological parameters were those related with visuo-spatial and perceptual functions normally related with the right hemisphere. At this point, the results derived from node performance analysis introduce a complementary explanation of the recovery process taking place within the brain. As shown in Fig. 4, those nodes that we define as "recovered" are more present in the delta band, showing that the therapy is especially efficient at low frequencies. In the alpha band, we do not observe such a good rehabilitation, specifically at the local activity. This later point could indicate that the network reorganization suggested by the global parameters could be a consequence of a reassignment of weights at the local activity.

Some computational models have studied the effect of damage and posterior recovery of brain network characteristics after injury. The work by Butz et al. (2009) addressed a very interesting question, how rehabilitation strategies must be designed (continuous or paused) to take full advantage of plasticity according to stimulations and comparing adult with juvenile networks. Modelling network damage is one of the best possibilities that graph theory offers, as shown, for example, in the works by Honey and Sporns (2008) and Alstott et al. (2009) in acquired brain injury, and Stam et al. (2009) in Alzheimer's disease. Traditionally, two different network alterations are modelled: a) the network damage is introduced at random by decreasing/increasing edge strength (or even removing edges), and b) the damage is targeted toward the more connected nodes. In the work by Alstott et al. (2009), the authors computationally study the effects of a localized structural lesion on the network, where lesion is implemented in two ways: a) sequential single node deletions (random and targeted) and localized area removal, and b) by removing all nodes and their connections within a spatially defined region around a central location. As shown by the authors, lesions along the cortical midline, the temporo-parietal junction and the frontal cortex, result in the largest and more widespread effects on functional connectivity. Also, lesions affect the coupling between regions outside the lesion itself, including the contralateral hemisphere. Honey and Sporns (2008) investigated the relationship between inter and intra regional couplings using two dynamical cortical models. Their results showed that high-degree nodes produce the largest and most widespread effects on cortico-cortical interactions. This result seems to be common in all models studying the effect of damage. Nakamura et al. (2009) have examined network properties following a similar experimental design as our study. Their results revealed that during recovery the network

begins to approximate what is observed in healthy controls. However, from our point of view, some questions are missing in this study: a) the decomposition into spectral bands, which reveals some valuable information, since, as we have seen, different bands are affected differently by injury and recovery, and b) the relation between changes in the topological parameters and those in cognitive evaluation.

Our experimental results show that TBI has different consequences in the delta and alpha bands. In the former, it is associated with an overall increase of synchronization, in the latter with a general decrease. Therefore, a network model must take into account both different behaviours. Structural changes are more focused in alpha based-functional connectivity. The evolution of the absolute values of the network parameters goes in the direction of the control group; also we found statistically significant variations of the normalized network parameters. This fact reveals that the modification of the functional network after recovery does not follow a random reorganization or, in other words, the recovery at the alpha band does not occur at all brain regions with the same probability. When a targeted evolutionary model is considered, the numerical results fit with the reorganization of the network suggested by the experimental results in the alpha band. Specifically, the targeted model has to take into account the fact that those links with higher activity need to increase their relevance in the network in order to recover the activity of the control group. On the contrary, a targeted model that diminishes the relative difference between network edges would fail in reproducing the evolution towards the healthy state after recovery. Our results show that the contrasting model fits the observed data better than the unifying model, indicating that the functional connectivity recovery in alpha band follows a plasticity principle where those links with higher activity play a fundamental role in recovery.

Concerning the delta band, we observe that neither the contrasting nor the unifying model is able to reproduce the changes observed in this band, which indicates that the delta band does not follow the same recovery process as the alpha band.

Finally, it is worth mentioning the interplay between changes observed in the delta and alpha bands and its possible implications. The energetic cost *EC* is an intuitive parameter that has great implications over the system and its dynamical behaviour, since it is related to the energy consumption of a physical information-processing system (Buzsaki, 2006). On one hand, delta-based networks experiment a hyper-synchronization effect after TBI, producing an overcharge of the network where energetic cost increases. On the other hand, the impact of TBI on alpha-based network results in a hypo-synchronization effect, decreasing the energetic cost of the functional network. This reduction leads to a decrease of the clustering *C* and an increase of the path length *L*, both changes leading to a worsening of the information transmission properties of the network. In the post condition, topological parameters converge to healthy controls, as it is the case of delta-band. Nevertheless, in this case, the increasing of energetic cost is a signal of recovering activity. Literature have yet documented the heterogeneity of networks depending on the spectral band considered (Palva et al., 2009; Bassett and Bullmore, 2009). Nevertheless, our results show that the overcharge observed in delta-based networks, and the disconnection found in alpha-based networks could follow a principle of balance-optimization of energetic cost, lost after TBI. It is not interesting to have neither minimal nor maximal energetic consumption, but having an optimal relationship between them, understanding optimal in terms of a reference established by healthy human brain networks. Although the energetic cost of the network is a parameter defining topological characteristics, it is closely related to the physical–anatomical measures in the brain. Individual or assemblies of physically close neurons have a higher probability of being connected than spatially remote neurons or regions (Braitenberg and Schüz, 1998; Hellwig, 2000; Cherniak, 1994). Many aspect of the brain anatomy can be explained considering the principle of minimising axonal wiring-volume or metabolic running cost (Chklovskii et al., 2002; Klyachko and Stevens, 2003; Buzsáki et al., 2004) since larger axonal projections are more material and energetically expensive (Cherniak et al., 2004). However, more recent results have shown that the neuroanatomical connectivity may not always be associated to an optimal distribution of the network connections (Kaiser and Hilgetag, 2006).

Our results show that the functional networks associated to the healthy group are those with a more balanced equilibrium between the network parameters of the delta and alpha bands (i.e., strength, shortest path, efficiency, energetic cost and clustering). It also seems that a trade-off between the synchronized activities of these two spectral bands has occurred to reach an optimal information-processing system, being the principle, we hypothesize in this work, that leads the plasticity process to the recovery of the acquired brain injury.

Acknowledgments

This work was supported by MADRI.B (CAM i+d+I project), Obra Social CajaMadrid, MAPFRE 2008 and IMSERSO (07-2008), the Spanish Ministry of Science and Technology (FIS2009-07072), and by the Community of Madrid under the R&D Program of activities MODELICO-CM/S2009ESP-1691. We are grateful to S. Aurtenetxe, O. Demuynck, J. García-Pacios, and D. del Rio for their generous help. We would like to thank Dr. Juan Manuel Muñoz Céspedes, who led this study. His ideas and personality will always be with us.

References

Achard, S., Bullmore, E., 2007. Efficiency and cost of economical brain functional networks. PLoS Comput. Biol. 3 (2), e17.
Aertsen, A., Gerstein, G.L., Habib, M.K., Palm, G., 1989. Dynamics of neuronal firing correlation: modulation of effective connectivity. Journal of Neurophysiology 61, 900–917.
Alstott, J., Breakspear, M., Hagmann, P., Cammoun, L., Sporns, O., 2009. Modeling the impact of lesions in the human brain. PLoS Comput. Biol. 5–6.
Bartolomei, F., Bosma, I., Klein, M., Baayen, J.C., Reijneveld, J.C., Postma, T.J., Heimans, J.J., van Dijk, B.W., de Munck, J.C., de Jongh, A., Cover, K.S., Stam, C.J., 2006a. Disturbed functional connectivity in brain tumour patients: evaluation by graph analysis of synchronization matrices. Clin. Neurophysiol. 117, 2039–2049.
Bartolomei, F., Bosma, I., Klein, M., Baayen, J.C., Reijneveld, J.C., Postma, T.J., Heimans, J.J., van Dijk, B.W., de Munck, J.C., de Jongh, A., Cover, K.S., Stam, C.J., 2006b. How do brain tumors alter functional connectivity? A magnetoencephalography study. Ann. Neurol. 59, 128–138.
Basset, D.S., Bullmore, E.T., Meyer-Lindenberg, A., Apud, J.A., Weinberger, D.R., Coppola, R., 2009. Cognitive fitness of cost-efficient brain functional networks. Proc. Natl Acad. Sci. USA 106 (28), 11747–11752 (Jul 14).
Bassett, D.S., Bullmore, E.T., 2009. Human brain networks in health and disease. Curr. Opin. Neurol. 22 (4), 340–347.
Beason-Held, L.L., Kraut, M.A., Resnick, S.M., 2009. Stability of default-mode network activity in the aging brain. Brain Imaging Behav. 3 (2), 123–131.
Boccaletti, S., Latora, V., Moreno, Y., Chavez, M., Hwang, D.U., 2006. Complex networks: structure and dynamics. Phys. Rep. 424, 175–308.
Bosma, I., Douw, L., Bartolomei, F., Heimans, J.J., van Dijk, B.W., Postma, T.J., et al., 2008. Synchronized brain activity and neurocognitive function in patients with low-grade glioma: a magnetoencephalography study. Neurooncology 10, 734–744.
Braitenberg, V., Schüz, A., 1998. Cortex: Statistics and Geometry of Neuronal Connectivity. Springer, Berlin.
Bressler, S., 2002. Understanding cognition through large-scale cortical networks. Curr. Dir. Psychol. Sci. 11, 58–61.
Brookes, M.J., Gibson, A.M., Hall, S.D., Furlong, P.L., Barnes, G.R., Hillebrand, A., Singh, K.D., Holliday, I.E., Francis, S.T., Morris, P.G., 2005. GLM-beamformer method demonstrates stationary field, alpha ERD and gamma ERS co-localisation with fMRI BOLD response in visual cortex. Neuroimage 26, 302–308.
Bullmore, E., Sporns, O., 2009. Complex brain networks: graph theoretical analysis of structural and functional systems. Nat. Rev. Neurosci. 10 (4), 312.
Buonomano, D.V., Merzenich, M.M., 1998. Cortical plasticity: from synapses to maps. Annu. Rev. Neurosci. 21, 149–186.
Butz, M., van Ooyen, A., Worgotter, F., 2009. A model for cortical rewiring following deafferentation and focal stroke. Front. Comput. Neurosci. 3, 10.
Buzsaki, G., 2006. Rhythms of the Brain. Oxford University Press, New York.
Buzsáki, G., Geisler, C., Henze, D.A., Wang, X.J., 2004. Interneuron diversity series: circuit complexity and axon wiring economy of cortical interneurons. Trends Neurosci. 27 (4), 186–193.

Campo, P., Poch, C., Parmentier, F.B.R., Moratti, S., Elsley, J.V., Castellanos, N.P., Ruiz-Vargas, J.M., Pozo, F., Maestú, F., 2010. Oscillatory activity in prefrontal and posterior regions during implicit letter-location binding. Neuroimagen. 49, 2807–2815.
Castellanos, N.P., Paul, N., Ordoñez, V.E., Demuynck, O., Bajo, R., Campo, P., Bilbao, A., Ortiz, del Pozo, F., Maestú, F., 2010. Reorganization of functional connectivity as a correlate of cognitive recovery in acquired brain injury. Brain 133, 2365–2381.
Cherniak, C., 1994. Component placement optimization in the brain. J. Neurosci. 14 (4), 2418–2427.
Cherniak, C., Mokhtarzada, Z., Rodriguez-Esteban, R., Changizi, K., 2004. Global optimization of cerebral cortex layout. Proc. Natl Acad. Sci. USA 101 (4), 1081–1086.
Chklovskii, D.B., Schikorski, T., Stevens, C.F., 2002. Wiring optimization in cortical circuits. Neuron 34 (3), 341–347.
Cicerone, K.D., Dahlberg, C., Kalmar, K., Langenbahn, D.M., Malec, J.F., Bergquist, T.F., et al., 2000. Evidence-based cognitive rehabilitation: recommendations for clinical practice. Phys. Med. Rehab. 81, 1596–1615.
Cicerone, K.D., Dahlberg, C., Malec, J.F., Langenbahn, D.M., Felicetti, T., Kneipp, S., Ellmo, W., Kalmar, K., Giacino, J.T., Harley, J.P., Laatsch, L., Morse, P.A., Catanese, J., 2005. Evidence-based cognitive rehabilitation: updated review of the literature from 1998 through 2005. Arch. Phys. Med. Rehabil. 86 (8), 1681–1692.
Cullen, N., Chundamala, J., Bayley, M., Jutai, J., et al., 2007. The efficacy of acquired brain injury rehabilitation. Brain Inj. 21 (2), 113–132.
Dall'Asta, L., Barrat, A., Barthélemy, M., Vespignani, A., 2006. Vulnerability of weighted networks. J. Stat. Mech. P04006.
Damoiseaux, J.S., Rombouts, S.A., Barkhof, F., Scheltens, P., Stam, C.J., Smith, S.M., Beckmann, C.F., 2006. Consistent resting-state networks across healthy subjects. Proc. Natl Acad. Sci. USA 103 (37), 13848–13853.
Deuker, L., Bullmore, E.T., Smith, M., Christensen, S., Nathan, P.J., Rockstroh, B., Basset, D.S., 2009. Reproducibility of graph metrics of human brain functional networks. Neuroimage. 47 (4), 1460–1468.
Dijkstra, E.W., 1959. A note on two problems in connection with graphs. Numer. Math. 1, 269–271.
Douw, L., Baayen, H., Bosma, I., Klein, M., Vandertop, P., Heimans, J., et al., 2008. Treatment-related changes in functional connectivity in brain tumor patients: a magnetoencephalography study. Exp. Neurol. 212, 285–290.
Fries, P., 2005. A mechanism for cognitive dynamics: neuronal communication through neuronal coherence. Trends Cogn. Sci. 9 (10), 474–480.
Fries, P., 2009. The model- and the data-gamma. Neuron 64 (5), 601–602.
Friston, K.J., Tononi, G., Reeke Jr., G.N., Sporns, O., Edelman, G.M., 1994. Value-dependent selection in the brain: simulation in a synthetic neural model. Neuroscience 59 (2), 229–243.
Gasser, T., Bacher, P., Mocks, J., 1982. Transformations towards the normal distribution of broad band spectral parameters of the EEG. Electroencephalogr. Clin. Neuropshysiol. 53, 119–124.
Gerloff, C., Bushara, K., Sailer, A., Wassermann, E.M., Chen, R., Matsuoka, T., Waldvogel, D., Wittenberg, G.F., Ishii, K., Cohen, L.G., Hallett, M., 2006. Multimodal imaging of brain reorganization in motor areas of the contralesional hemisphere of well recovered patients after capsular stroke. Brain 129 (Pt 3), 791–808.
Gong, Y., Zhang, Z., 2009. Global robustness and identifiability of random, scale-free, and small-world networks. Ann. NY Acad. Sci. 1158, 82–92.
Grinsted, A., Moore, J.C., Jevrejeva, S., 2004. Application of the cross wavelet transform and wavelet coherence to geophysical time series. Nonlinear Process. Geophys. 11, 561–566.
Guggisberg, A.G., Honma, S.M., Am, Findlay, Dalal, S.S., Kirsch, H.E., Berger, M.S., et al., 2008. Mapping functional connectivity in patients with brain lesions. Ann. Neurol. 63, 193–203.
Guimerà, R., Amaral, L.A., 2005. Cartography of complex networks: modules and universal roles. J. Stat. Mech. P02001.
He, Y., Evans, A., 2010. Graph theoretical modeling of brain connectivity. Curr. Opin. Neurol. 23 (4), 341–350.
Hellwig, B., 2000. A quantitative analysis of the local connectivity between pyramidal neurons in layers 2/3 of the rat visual cortex. Biol. Cybern. 82 (2), 111–121.
Honey, C.J., Sporns, O., 2008. Dynamical consequences of lesions in cortical networks. Hum. Brain Mapp. 29, 802–809.
Kaiser, M., Hilgetag, C.C., 2006. Nonoptimal component placement, but short processing paths, due to long-distance projections in neural systems. PLoS Comput. Biol. 2 (7), e95.
Kelly, C., Foxe, J.J., Garavan, H., 2006. Patterns of normal human brain plasticity after practice and their implications for neurorehabilitation. Arch. Phys. Med. Rehabil. 87, S20–S29.
Klyachko, V.A., Stevens, C.F., 2003. Connectivity optimization and the positioning of cortical areas. Proc. Natl Acad. Sci. USA 100 (13), 7937–7941.
Korzeniewska, A., Manczak, M., Kaminski, M., Blinowska, K., Kasicki, S., 2003. Determination of information flow direction among brain structures by a modified directed transfer function (dDTF) method. J. Neurosci. Meth. 125, 195–207.
Latora, V., Marchiori, M., 2001. Efficient behavior of small-world networks. Phys. Rev. Lett. 87, 198701.
Lewine, J.D., Davis, J.T., Sloan, J.H., Kodituwakku, P.W., Orrison Jr., W.W., 1999. Neuromagnetic assessment of pathophysiologic brain activity induced by minor head trauma. AJNR Am. J. Neuroradiol. 20 (5), 857–866.
Lewine, J.D., Davis, J.T., Bigler, E.D., Thoma, R., Hill, D., Funke, M., Sloan, J.H., Hall, S., Orrison, W.W., 2007. Objective documentation of traumatic brain injury subsequent to mild head trauma: multimodal brain imaging with MEG, SPECT, and MRI. J. Head Trauma Rehabil. 22 (3), 141–155.
Li, Y., Liu, Y., Li, J., Qin, W., Li, K., Yu, C., Jiang, T., 2009. Brain anatomical network and intelligence. PLoS Comput. Biol. 5 (5), e1000395 (May).
Meunier, D., Achard, S., Morcom, A., Bullmore, E., 2009. Age-related changes in modular organization of human brain functional networks. Neuroimage 44 (3), 715–723.
Micheloyannis, S., Pachou, E., Stam, C.J., Vourkas, M., Erimaki, S., Tsirka, V., 2006. Using graph theoretical analysis of multi channel EEG to evaluate the neural efficiency hypothesis. Neurosci. Lett. 402 (3), 273–277 (Jul 24).
Nakamura, T., Hillary, F.G., Biswal, B.B., 2009. Resting network plasticity following brain injury. PLoS ONE 14, 4–12.
Palva, S., Monto, S., Palva, J.M., 2009. Graph properties of synchronized cortical networks during visual working memory maintenance. Neuroimage 49 (4), 3257–3268.
Palva, J.M., Monto, S., Kulashekhar, S., Palva, S., 2010a. Neuronal synchrony reveals working memory networks and predicts individual memory capacity. Proc. Natl Acad. Sci. USA 107 (16), 7580–7585.
Palva, S., Monto, S., Palva, J.M., 2010b. Graph properties of synchronized cortical networks during visual working memory maintenance. Neuroimage 49 (4), 3257–3268.
Park, N.W., Ingles, J.L., 2001. Effectiveness of attention rehabilitation after an acquired brain injury: a meta-analysis. Neuropsychology 15 (2), 199–210.
Pivik, R.T., Broughton, R.J., Coppola, R., Davidson, R.J., Fox, N., Nuwer, M.R., 1993. Guidelines for the recording and quantitative analysis of electroencephalographic activity in research contexts. Psychophysiology 30, 547–558.
Rohling, M.L., Faust, M.E., Beverly, B., Demakis, G., 2005. Effectiveness of cognitive rehabilitation following acquired brain injury: a meta-analytic re-examination of Cicerone et al.'s (2000, 2005) systematic reviews [Review]. Neuropsychology. 2009; 23 (1):20–39.
Schnitzler, A., Gross, J., 2005. Normal and pathological oscillatory communication in the brain. Nat. Rev. Neurosci. 6, 285–296.
Schreiber, T., Schmitz, A., 2000. Surrogate time series. Physica D 142, 646–652.
Singer, W., 1999. Neuronal synchrony: a versatile code for the definition of relations? Neuron 24, 49–65.
Singer, W., 2009. Distributed processing and temporal codes in neuronal networks. Cogn. Neurodyn. 3 (3), 189–196.
Stam, C.J., 2010. Characterization of anatomical and functional connectivity in the brain: a complex networks perspective. Int. J. Psychophysiol. 77 (3), 186–194.
Stam, C.J., de Haan, W., Daffertshofer, A., Jones, B.F., Manshanden, I., van Cappellen van Walsum, A.M., Montez, T., Verbunt, J.P., de Munck, J.C., van Dijk, B.W., Berendse, H.W., Scheltens, P., 2009. Graph theoretical analysis of magnetoencephalographic functional connectivity in Alzheimer's disease. Brain 132 (Pt 1), 213–224.
Theiler, J., Eubank, S., Longtin, A., Galdrikian, B., Farmer, D., 1992. Testing for nonlinearity in time series: the method of surrogate data. Physica D 58, 77–94.
Tononi, G., Sporns, O., Edelman, G.M., 1994. A measure for brain complexity: relating functional segregation and integration in the nervous system. PNAS 91, 5033–5037.
Torrence, C., Compo, G.P., 1998. A practical guide to wavelet analysis. Bull. Am. Meteorol. Soc. 79, 61–78.
Van den Heuvel, M., Stam, C.J., Kahn, R.S., Hulshoff, E., 2009. Efficiency of functional brain networks and intellectual performance. J. Neurosci. 29 (23), 7619–7624.
Varela, F., Lachaux, J.P., Rodriguez, E., Martinerie, J., 2001. The brainweb: phase synchronization and large-scale integration. Nat. Rev. Neurosci. 2, 229–239.
Watts, D.J., Strogatz, S.H., 1998. Collective dynamics of 'small-world' networks. Nature 393 (6684), 440–442.